ACS Catalysis

Research Article

pubs.acs.org/acscatalysis

Unintuitive Inverse Dependence of the Apparent Turnover Frequency on Precatalyst Concentration: A Quantitative Explanation in the Case of Ziegler-Type Nanoparticle Catalysts Made from $[(1,5\text{-COD})Ir(\mu\text{-}O_2C_8H_{15})]_2$ and $AlEt_3$

Adam B. Crooks,[†] Kuang-Hway Yih,[†] Long Li,[‡,§] Judith C. Yang,[‡] Saim Özkar,[∥] and Richard G. Finke*[,†]

[†]Department of Chemistry, Colorado State University, Fort Collins, Colorado 80523, United States

[‡]University of Pittsburgh, Pittsburgh, Pennsylvania 15261, United States

[§]RJ Lee Group, Inc., 350 Hochberg Road, Monroeville, Pennsylvania 15146, United States

[∥]Department of Chemistry, Middle East Technical University, 06800 Ankara, Turkey

Supporting Information

ABSTRACT: The Ziegler-type hydrogenation precatalyst dimer, $[(1,5\text{-COD})Ir(\mu\text{-}O_2C_8H_{15})]_2$ (1,5-COD = 1,5-cyclooctadiene; $O_2C_8H_{15}$ = 2-ethylhexanoate) plus added $AlEt_3$ stabilizer has recently been shown to form $AlEt_3$-stabilized, Ziegler-type $Ir(0)_{\sim 4-15}$ nanoparticles initially, which then grow to larger Ziegler-type $Ir(0)_{\sim 40-50}$ nanoparticles during the catalytic hydrogenation of cyclohexene (Alley, W. M.; Hamdemir, I. K.; Wang, Q.; Frenkel, A. I.; Li, L.; Yang, J. C.; Menard, L. D.; Nuzzo, R. G.; Özkar, S.; Johnson, K. A.; Finke, R. G. *Inorg. Chem.* **2010**, 49, 8131−8147). An interesting observation for this Ziegler-type nanoparticle catalyst system is that the apparent TOF ($TOF_{app} = k_{obs}/[Ir]$) for cyclohexene hydrogenation *increases* with *decreasing* concentration of the precatalyst, [Ir] (defined as $2[\{(1,5\text{-COD})Ir(\mu\text{-}O_2C_8H_{15})\}_2]$, that is, twice the starting precatalyst concentration since that dimer contains 2 Ir). A perusal of the literature reveals that such an intuitively backward, inverse relationship between the apparent turnover frequency, TOF_{app}, and the concentration of precatalyst or catalyst has been seen at least eight times before in other, disparate systems in the literature. However, this effect has previously never been satisfactorily explained, nor have the mixed, sometimes opposite, explanations offered in the literature been previously tested by the disproof of all reasonable alternative explanations/mechanistic hypotheses. Herein, five alternative mechanistic explanations have been tested via kinetic studies, Z-contrast STEM microscopy of the nanoparticle product sizes, and other evidence. Four of the five possible explanations have been ruled out en route to the finding that the only mechanism of the five able to explain all the evidence, as well as to quantitatively curve-fit the inverse TOF_{app} vs [Ir] data, is a prior, dissociative equilibrium, in which $x \approx 3$ equiv of the surface-bound, AlR_3-based nanocluster stabilizer is dissociated, $Ir(0)_n{\cdot}[AlEt_3]_m \rightleftarrows xAlEt_3 + Ir(0)_n{\cdot}[AlEt_3]_{m-x}$, with the resulting, more coordinatively unsaturated $Ir(0)_n{\cdot}[AlEt_3]_{m-x}$ being the faster, kinetically dominant catalyst. The implication is that such unusual, inverse TOF_{app} vs [precatalyst or catalyst] concentration observations in the literature are, more generally, likely just unintentional, unwitting measurements of a component of the rate law for such systems. The results herein are significant (i) in providing the first quantitative, disproof-tested explanation for the inverse TOF_{app} vs [precatalyst or catalyst] observation; (ii) in providing precedent and, therefore, a plausible explanation for the eight prior examples of this phenomenon in the literature; and (iii) in demonstrating for one of those additional eight literature cases, a commercial cobalt-based polymer hydrogenation catalyst, that the prior dissociative equilibrium uncovered herein can also quantitatively fit the inverse TOF_{app} vs [precatalyst] data for that case, as well. The results herein are additionally significant (iv) in making apparent that the rigorous interpretation of any TOF requires that the rate law for the processes under study be known, a point that bears heavily on the confusion and current controversy in the literature over the proper use of the "TOF" concept; (v) in making apparent the usefulness and value of the TOF_{app} concept employed herein; and (vi) in uncovering the insight that the true, most active catalyst present in $AlEt_3$-stabilized, Ziegler-type $Ir(0)_n$ nanoparticle catalysts is the more coordinatively unsaturated Ziegler-type $Ir(0)_n{\cdot}[AlEt_3]_{m-x}$ nanoparticle formed from the dissociative loss of ~3 $AlEt_3$.

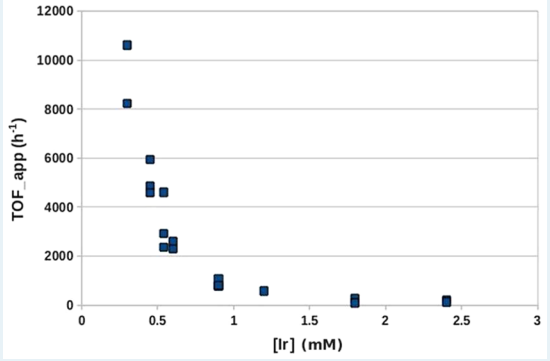

KEYWORDS: *turnover frequency, Ziegler-type nanoclusters, hydrogenation catalysis, kinetics and mechanism, inverse dependence of turnover frequency on catalyst concentration*

Received: February 19, 2015
Revised: April 9, 2015
Published: April 30, 2015

DOI: 10.1021/acscatal.5b00347
ACS Catal. 2015, 5, 3342−3353

INTRODUCTION

Ziegler-type hydrogenation catalysts, formed from nonzero valent Group 8−10 transition metal compounds (industrially typically Co or Ni) combined with trialkylaluminum cocatalyst, are important industrial catalysts, one used, for example, to hydrogenate >1.7×10^5 metric tons of styrenic block copolymers (Figure 1) annually.[1−4] (Ziegler−Natta *polymerization* catalysts are different and are not the subject of this paper.)

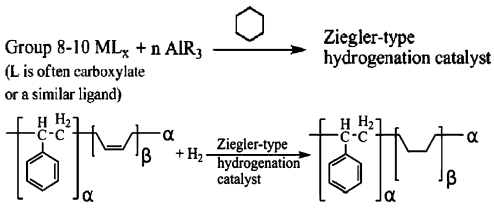

Figure 1. Formation of the Ziegler-type catalysts and their hydrogenation of a styrenic block copolymer.

We recently reported the characterization of model iridium Ziegler-type nanoparticle hydrogenation catalysts made from the crystallographically characterized precatalyst [(1,5-COD)Ir(μ-$O_2C_8H_{15}$)]$_2$ (Figure 2) plus $AlEt_3$ using a variety of analytical

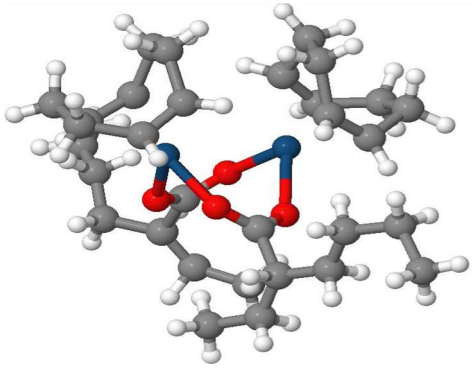

Figure 2. Structure of the dimeric [(1,5-COD)Ir(μ-$O_2C_8H_{15}$)]$_2$ precursor.[2] The coordination of the 1,5-COD group to each Ir has been removed for clarity. Blue = Ir, red = O, gray = C, white = H.

techniques, including Z-contrast scanning transmission electron spectroscopy (STEM); X-ray absorption fine structure (XAFS) spectroscopy; matrix-assisted laser desorption/ionization (MALDI) mass spectrometry; and, importantly, kinetic studies.[5] That study shows that the initial catalytically active solutions contain a broad range of Ir species with initially noncrystalline structures. An estimated mean $Ir_{\sim 4-15}$ subnanometer particle is seen initially post-$AlEt_3$ addition to the [(1,5-COD)Ir(μ-$O_2C_8H_{15}$)]$_2$ precatalyst.[5] However, during catalytic hydrogenation, larger and more active $Ir_{\sim 40-50}$ Ziegler nanoparticles develop (Scheme 1).

We also studied the high thermal stability[6] and nature of the stabilizing species in Ziegler-type hydrogenation catalysts,[7] with a focus on the ∼50-year-old question of whether such catalysts are homogeneous (i.e., homotopic,[8] defined by Crabtree as possessing a single type of catalytically active site)[9] or heterogeneous $M(0)_n$ nanoparticles (i.e., heterotopic,[8] defined by Crabtree as possessing multiple types of active sites). The evidence is compelling that heterogeneous (i.e., heterotopic[5]) Ziegler-type nanoparticles are formed, nanoparticles which are unusual "weakly ligated with labile ligands", since the only potential ligands/

Scheme 1. Generalized Scheme Proposed First Elsewhere[1] For The Formation Of Ziegler-Type $Ir(0)_n$ Nanoparticles from [(1,5-COD)Ir(μ-$O_2C_8H_{15}$)]$_2$ Plus $AlEt_3$, for Their Transformation to Larger Nanoparticles, and for Their Resultant Olefin Hydrogenation Catalysis[a]

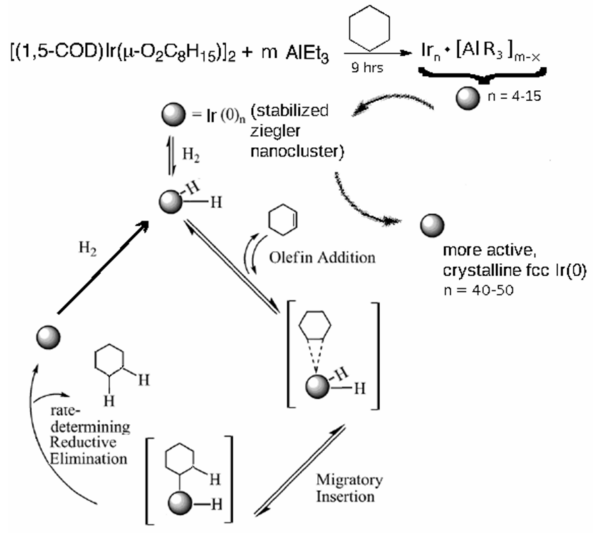

[a]As detailed elsewhere, the order of olefin addition and oxidative addition of H_2 are not known with certainty.

stabilizers are cyclohexane, cyclohexene, the added Lewis acid $AlEt_3$,[10] or species derived from the $AlEt_3$.[7] Such weakly ligated/labile ligand nanoparticles are of current interest, since they tend to exhibit higher catalytic activity.[5,11] The Ir(0) Ziegler-type nanoparticles studied herein are also unusual in that they are hydrocarbon-soluble as well as thermally stable up to 200 °C in dodecane for >30 min when ≥3 equiv of $AlEt_3$ is present.

The Observation of an Inverse TOF_{app} vs Precatalyst Concentration Dependence. Kinetic studies of the [(1,5-COD)Ir(μ-$O_2C_8H_{15}$)]$_2$ plus $AlEt_3$-derived system, obtained as part of the present work and shown in Figure 3 (see the

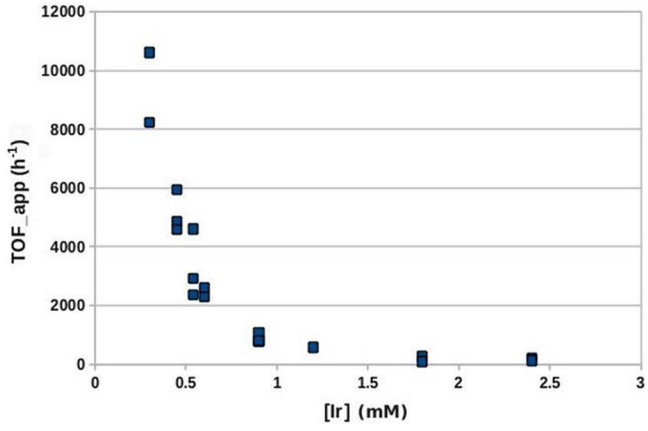

Figure 3. Observed inverse trend where higher apparent turn over frequencies are observed at lower [Ir] concentrations, where [Ir] = 2 times the starting [(1,5-COD)Ir(μ-$O_2C_8H_{15}$)]$_2$ concentration. The data will be curve-fit and further analyzed in Figure 8 (vide infra).

Experimental Section and the Results and Discussion, vide infra), reveal that the apparent turn over frequency,[12] $TOF_{app} = k_{obs}$/[precatalyst], *increases* with *decreasing* [Ir]. Understanding this

DOI: 10.1021/acscatal.5b00347
ACS Catal. 2015, 5, 3342−3353

inverse dependence of the TOF_{app} on the precatalyst concentration is important because the *true TOF* will by definition be a constant "for a given metal, metal oxide, or metal sulfide in a given reaction at specified reaction conditions."[12] That is, the fact that the TOF_{app} in Figure 3, for example, is not a constant means that we should not be calling it a (true) "TOF". The kinetic implication here is that a nonconstant TOF_{app} means that there is some aspect of the underlying rate law that is ill-understood so that what one is actually measuring is an apparent rate constant, k_{obs}, that might, for example, still contain hidden concentration terms. Then, when one turns that k_{obs} into a "TOF" value, one needs to realize that it should be labeled an *apparent* TOF value, $TOF_{app} = k_{obs}/[\text{precatalyst}]$, and not a (true) $TOF = k/[\text{catalyst}]$, unless one has demonstrated that k is a true, unchanging, rate *constant*. Indeed, such nonconstant TOF_{app} values that, for example, vary inversely with the [precatalyst or catalyst] must, in a more general sense, be somewhat unwitting measurements of the true rate law of the underlying, catalytic system. Hence, one of the simplest but most important parts of this paper is just the use of TOF_{app} and its distinction from the (true) TOF.

Inverse TOF_{app} vs precatalyst concentration dependencies have been reported at least eight times before (vide infra), including in supported catalytic systems,[13] but have (i) previously never been unequivocally tested or explained, since (ii) the possible explanations and underlying mechanisms have not been previously collected as part of a single study until now. This, in turn, means that (iii) a rigorous explanation, supported by the attempted disproof of each plausible literature hypothesis plus the hypotheses constructed as part of the present study (vide infra), has not appeared previously.

Literature Observations of an Inverse Dependence of TOF_{app} vs Precatalyst Concentration Leading to Five Alternative Mechanistic Hypotheses. *The Bimolecular Agglomeration Hypothesis.* An inverse relationship has been observed in the $Co(acac)_2$ plus $AlEt_3$ Ziegler-type hydrogenation catalyst system studied by Shmidt and co-workers[14] (Figure 4).

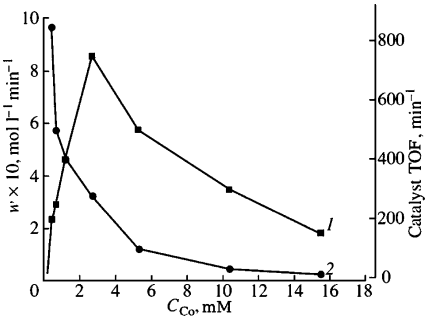

Figure 4. Shmidt and co-workers' study of the dependence of the TOF (right axis) and the rate (left axis, given as w) of 1-hexene hydrogenation in heptane on the initial $[Co(acac)_2]$ of the $Co(acac)_2/AlEt_3$ precatalyst system.[15] Reproduced with permission from ref 15. Copyright 2005, Elsevier. Note, however, that the x-axis has been corrected to the indicated millimolar units, and the right-most, y-axis to TIF (vs the original figure, which has M and TON, respectively[15]), since the authors of ref 15 informed us about those misprints in their original figure.[15]

In their study, Shmidt and co-workers interpreted the inverse relationship as evidence for a heterogeneous catalyst, arguing that if the system was a homogeneous catalyst, then it would have shown an invariant TOF as a function of concentration. We have since shown that $Co_{\sim 4}$ subnanometer clusters are formed in a $Co(\text{neodecanoate})_2/AlEt_3$ precatalyst system, clusters known to provide the currently most active industrial Ziegler-type hydrogenation catalyst.[3] Noteworthy is that the results in Figure 4 mirror those in Figure 3 that are analyzed herein, a close parallel which lends credence to the primary data in both studies.

Shmidt and co-workers postulated that the observed inverse trend was caused by particle agglomeration (a lack of agglomeration at low concentrations of cobalt, which is consistent with their interpretation, was observed),[15] but definitive kinetic and mechanistic studies supporting (or refuting) that supposition are lacking.

Bimolecular catalyst agglomeration with concomitant catalyst deactivation has been used to rationalize the [catalyst] dependence in alcohol oxidation by Pd(0) studied by Steinhoff et al.[16] Indeed, catalyst deactivation by bimolecular agglomeration is a recurring explanation in the literature for inverse TOF_{app} vs concentration data. It is, therefore, a key hypothesis that will be tested for the $Ir(0)_n/AlEt_3$ Ziegler nanoparticle system examined herein. This alternative hypothesis is summarized in Scheme 2,

Scheme 2. Bimolecular Agglomeration and Reversible Fragmentation Hypotheses[a]

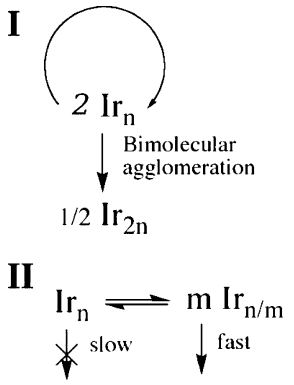

[a]The down arrows in part II connect to the catalytic cycle (which is, however, not shown, since it is unnecessary to illustrate this hypothesis).

part I. Discussed next is a reversible fragmentation/reagglomeration hypothesis, as shown in Scheme 2, part II.

The Concentration-Dependent Cluster Fragmentation Hypothesis. Sánchez-Delgado et al.[17] observed an inverse trend in styrene hydrogenation rates when starting with Os_4 clusters. They attributed this trend to a concentration-dependent fragmentation of the tetranuclear Os_4 subnanometer clusters into smaller nuclearity, more catalytically active clusters at lower concentrations of Os. Sánchez-Delgado et al.[17] considered the possibility that active Os_4 clusters could aggregate at higher concentration, but ruled out this possibility experimentally by performing a series of styrene hydrogenation control experiments. After the styrene hydrogenation, they failed to observe species larger than Os_4 by IR. Further, they found no catalytic activity when the osmium clusters ($H_3Os_4(CO)_{12}(I)$ and $H_4Os_4(CO)_{12}$) were supported on MgO (200),[17] a result that they attribute to ionic chemisorption of the cluster to the support (which thereby inhibits fragmentation).[18] The fragmentation postulate is, nevertheless, another alternative hypothesis that is considered as part of the present work. Scheme 2, part II, shows the concentration-dependent fragmentation hypothesis adapted to the current $Ir(0)_n$ system.

Palladium-catalyzed coupling reactions have exhibited an inverse TOF_{app} vs [Pd] trend, as well.[19−22] Two previously proposed

DOI: 10.1021/acscatal.5b00347
ACS Catal. 2015, 5, 3342−3353

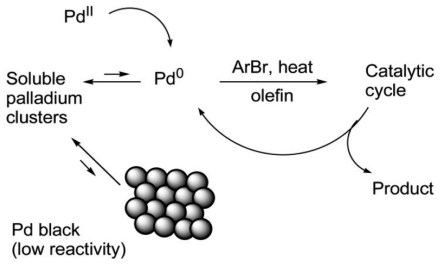

Figure 5. Scheme from Reetz and de Vries' study of Heck reactions with aryl bromides. Shown here is their proposed equilibrium fragmentation reaction scheme. The Pd concentration must be kept below 0.1 mol %; otherwise, Pd black is formed. Reproduced with permission from ref 20. Copyright 2004, RSC Publishing.

explanations, as illustrated in Figure 5, are (i) agglomerative formation of large unreactive $Pd(0)_n$ particles at high catalyst loadings, which then fragment to form active monomeric species;[19] and (ii) a fragmentation equilibrium between inactive $Pd(0)_n$ particles and catalytically active mononuclear[21] or binuclear $Pd(0)_{1-2}$ species. In what is basically another version of the mechanistic scheme part II shown back in Scheme 2, Le Chatlier's principle can then be invoked to explain that "the equilibrium shifts toward the lower-order species at lower concentrations".[20] Hence, agglomeration and fragmentation (as summarized back in Scheme 2), and as illustrated for Pd in Figure 5, once again arises as important hypotheses to be tested herein.

The Concentration-Dependent Size, Plus Size-Specific Catalytic Activity, Hypothesis. The underlying idea behind this next literature, alternative hypothesis is that there is a concentration-dependent nanoparticle size and size-dependent catalytic activity. If lower concentrations of precatalyst produced smaller particles,[23,24] and if those smaller particles were more catalytically active as has precedent[25] for *some* reactions,[26] then a size-specific catalytic activity could conceivably and in principle produce an inverse TOF_{app} vs [precatalyst] dependence.

This particular hypothesis has some precedent in Zhou et al.'s single-molecule fluorescence spectroscopy experiments on the Au_n-catalyzed reduction of resazurin to resorufin.[26] In that system, the catalytic activity per unit surface area increased for the smaller nanoparticles. Hence, the hypothesis of a concentration plus size-dependent catalytic activity needs to be added to the list of plausible hypotheses meriting scrutiny[27] as part of the present work.

The Insidious Impurity Hypothesis—Especially Trace Water in the Case of $AlEt_3$-Stabilized Ziegler-Type Nanoparticles. In general and for virtually every chemical system, there is nearly always the often perplexing alternative hypothesis that some "insidious impurity" is responsible for the observations at hand.[28] In the present case, trace water is a specific, potential impurity that is a quite plausible alternative hypothesis that must, therefore, also be considered. Any trace H_2O would tend to increase relative to the amount of decreasing [Ir] plus $AlEt_3$ as one goes to lower concentrations in the data shown back in Figure 3. In addition, it is known for the present Ir/$AlEt_3$ system that less $AlEt_3$ can give a faster nanoparticle catalyst (at least if there is still a minimum of 1.0 $AlEt_3$ present). Hence, trace water—that would react with $AlEt_3$ and thereby remove it—could, in principle, lead to a faster catalyst with decreasing [Ir precatalyst]. This alternative hypothesis does, however, depend on the (unknown) effect of the resultant alumoxane product, $-[(Al(Et)O)]_m-$, that would be produced from hydrolysis of the $AlEt_3$. In short, the "insidious H_2O impurity" hypothesis merits careful consideration and attempted disproof.

The Concentration-Dependent, Prior Equilibrium Hypothesis. Our intuition from the start has been that there is very likely just some *undetermined concentration dependence* in the rate law, connected to the catalyst in some mannter, for many if not most systems exhibiting the inverse TOF vs [precatalyst or catalyst] phenomenon. That is, in this alternative hypothesis, the turnover frequency being measured is just an apparent turnover frequency, TOF_{app}, so that the observed nonconstant TOF_{app} vs [precatalyst or catalyst] curves are a somewhat unwitting measurement of some concentration dependence contained within the more complete, albeit presently unknown, rate law. More specifically, a *concentration-dependent prior equilibrium* is a specific hypothesis that can at least in principle explain inverse TOF_{app} vs [precatalyst or catalyst] data.

Because prior equilibrium mechanisms are among the most common general mechanism in the chemical sciences, we further reasoned that an example that is at least somewhat illustrative of what is effectively an inverse k_{obs} vs [added reagent] effect must exist somewhere in the prior literature. Note what we are looking for here is a case in which the added reagent *is a reactant* and, therefore, on the left-hand side of the reaction arrow (as is a catalyst), so that a linear and *not the observed inverse* dependence on the [Reactant] is what one normally, intuitively *expects*.

A careful, additional literature search—now with an eye for what we were looking for—turned up a pedagogically illustrative example, one missed in all of the eight prior papers reporting an inverse "TOF" (i.e., really TOF_{app}) phenomenon. That example is the 1971 literature of Byrd and Wilmarth,[29] and a *Journal of Chemical Education* paper by Malin and co-workers,[30] in which their goal was to illustrate how a k_{obs} could have a somewhat unintuitive inverse dependence on a the concentration of a reactant.

Specifically, Malin et al. examined the reaction of the faint-yellow complex $Fe(CN)_5DMSO^{3-}$ with *N*-methylpyrazinium (MPz^+) to form the deep blue product $Fe(CN)_5MPz^+$. The kinetics of this reaction are easily followed via UV−vis at 655 nm. An inverse dependence of k_{obs} vs the added [reactant] = [MPz^+] is seen in this system (Figure 6). The proposed mechanism and associated rate law and resultant k_{obs}, shown in Scheme 3 quantitatively account for the observed inverse k_{obs} vs [MPz^+] dependence due to the equilibrium involving MPz^+. Specifically, the equation for k_{obs} in Scheme 3 teaches that at low [MPz^+], $k_{obs} = k_{-2}$, whereas at high [MPz^+], $k_{obs} = k_1$. Hence, when $k_{-2} > k_1$, as is the case for this system, then an inverse k_{obs} vs [MPz^+] plot as shown in Figure 6 should be—and is—seen.

In short, the k_{obs} vs concentration profile in Figure 6 has an obvious, quantitatively explainable inverse dependency once the full rate law is known. Hence, this broadly missed *Journal of Chemical Education* article[30] provides a very valuable example of where a concentration-dependent equilibrium, involving a reagent present in the reaction and, thus, in the rate law, gives rise to an initially unintuitive inverse dependence of k_{obs} on that [reagent]. If this had been a catalytic system, for which the $TOF_{app} \propto k_{obs}$, then an inverse TOF_{app} vs [reactant] would have been seen, illustrating how a concentration-dependent equilibrium can in a general way lead to such inverse dependencies. That said, since the Malin et al. example involves a reversible equilibrium at the end of the reaction (and not an equilibrium prior to the rate-determining step as in the TOF_{app} vs [Ir] example herein, vide infra), and since it is not a catalytic

DOI: 10.1021/acscatal.5b00347
ACS Catal. 2015, 5, 3342−3353

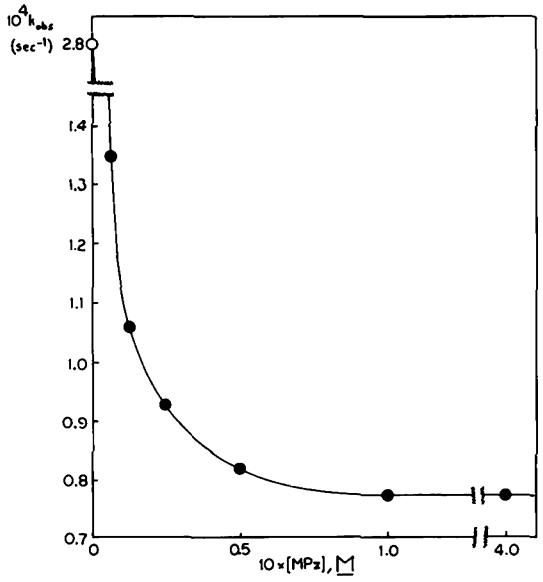

Figure 6. Concentration dependence of the observed rate constant, k_{obs}, on the dependence of *N*-methylpyranzium (MPz^+) in the substitution reaction on $Fe(CN)_5DMSO^{3-}$ in which MPz^+ replaces DMSO, as shown in Scheme 3. The title of this paper is "An Undergraduate Kinetics Experiment Demonstrating Unusual Behavior in k_{obs}".[30] Reproduced with permission from ref 30. Copyright 1977, ACS Publications.

Scheme 3. Two-Equilibrium-Step Mechanism Proposed by Malin et al.[30] Which Was Used (i) To Derive an Expression for k_{obs} Shown below, and Then (ii) To Quantitatively Fit the Observed Data, As Shown in Figure 6

$$Fe(CN)_5DMSO^{3-}(aq) \underset{k_{-1}}{\overset{k_1}{\rightleftharpoons}} Fe(CN)_5{}^{3-}(aq) + DMSO(aq)$$

$$MPz^+(aq) + Fe(CN)_5{}^{3-}(aq) \underset{k_{-2}}{\overset{k_2}{\rightleftharpoons}} Fe(CN)_5MPz^{2-}(aq)$$

$$k_{obs} = \frac{k_1k_2[MPz^+] + k_{-1}k_{-2}[DMSO]}{k_2[MPz^+] + k_{-1}[DMSO]}$$

reaction, the Malin et al. example serves only as a general precedent for the TOF_{app} vs [Ir] case analyzed herein.

In summary, an inverse TOF_{app} vs [precatalyst or catalyst] concentration effect has been reported at least eight times before in the literature. The concentration-dependent prior equilibrium hypothesis created as part of the present work, plus the four additional alternative hypotheses that result from that literature, are summarized in Table 1, along with key, testable observables expected for each hypothesis. The "concentration-dependent prior equilibrium" hypothesis is listed first in Table 1, since it will be the first hypothesis we subject to attempted disproof in what follows.

RESULTS AND DISCUSSION

The TOF_{app} vs [Ir] Kinetic Data. Catalytic cyclohexene hydrogenation reactions in cyclohexane solvent were run as detailed in the Experimental Section beginning with the precatalyst $[(1,5\text{-COD})Ir(\mu\text{-}O_2C_8H_{15})]_2$ plus $AlEt_3$ at a fixed $AlEt_3$/Ir ratio of 2.0, where an active, generally optimum catalyst is known to result.[5] The reactions were monitored as before[5] by the loss of H_2 pressure by a sensitive, ±0.01 psig pressure transducer. The hydrogenations were performed at a range of beginning precatalyst [Ir] concentrations [Ir] = 2[(1,5-COD)-Ir(μ-$O_2C_8H_{15}$)]$_2$, four of which are shown in Figure 7 just to illustrate the raw psig vs time data. The resultant TOF_{app} (1/(h*surface site)) vs [Ir] data are shown in Figure 8 (the same data as shown in Figure 3), but now with its curve-fit and analysis (vide infra). The inverse dependence of TOF_{app} with [Ir] is sizable, a factor of ~127-fold in TOF_{app} from its smallest to largest value.

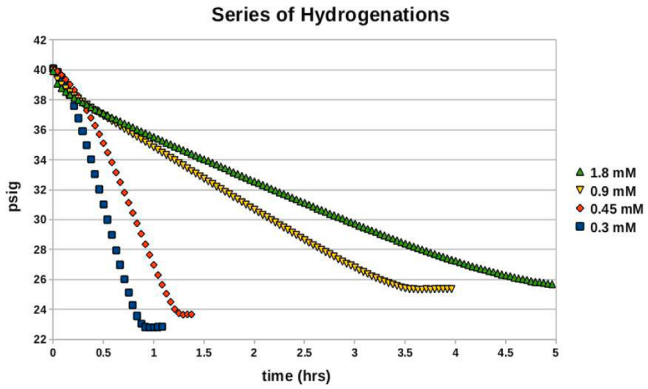

Figure 7. Representative catalytic hydrogenation kinetic data at four different concentrations of precatalyst ([Ir] = 0.3, 0.45, 0.9 and 1.8) and a fixed $AlEt_3$/Ir ratio of 2.0. The average hydrogen consumption over the period of catalytic activity was measured and defined as k_{obs}.

Each hypothesis summarized in Table 1 was then considered for its ability to explain both the kinetic data and the accompanying STEM data.

(1). The "Concentration-Dependent Prior Equilibrium Hypothesis" Hypothesis, Specifically a Dissociative $AlEt_3$ Prior Equilibrium. The kinetic and resultant mechanistic scheme underlying this hypothesis, written in a deliberately minimalistic

Table 1. An Overview Summary of the Five Hypotheses, The Relevant Literature, And Some Experimental Tests They Generate

hypothesis	relevant literature	experimental tests and expectations
1. concentration-dependent prior equilibrium hypothesis; specifically, an $AlEt_3$ stabilizer, prior dissociative equilibrium hypothesis	Malin et al.[30] precedent for an inverse k_{obs} vs [reactant]	kinetics of the $AlEt_3$ stabilizer dependence; no change expected in nanoparticle size with [$AlEt_3$] by STEM
2. bimolecular agglomeration hypothesis	Steinhoff et al.,[16] Shmidt et al.[15]	larger (less active) particles should be observable at higher [precatalyst] by STEM
3. concentration-dependent cluster fragmentation hypothesis	De Vries et al.,[21] Reetz et al.[20]	smaller particles expected at lower [precatalyst], some of which should be observable by STEM
4. concentration-dependent size with size-specific activity hypothesis	Zhou et al.,[26] Watzky et al.[23]	smaller, more active nanoparticles, formed at lower [precatalyst], some of which should be observable by STEM
5. insidious H_2O impurity hypothesis	Doll et al.[28] (re: the general "insidious impurity hypothesis")	at lower [catalyst], adventitious water is hypothesized to become more important, leading to a faster catalyst by reacting with $AlEt_3$ thereby removing it from the $Ir(0)_n$ nanoparticle surface

DOI: 10.1021/acscatal.5b00347
ACS Catal. 2015, 5, 3342−3353

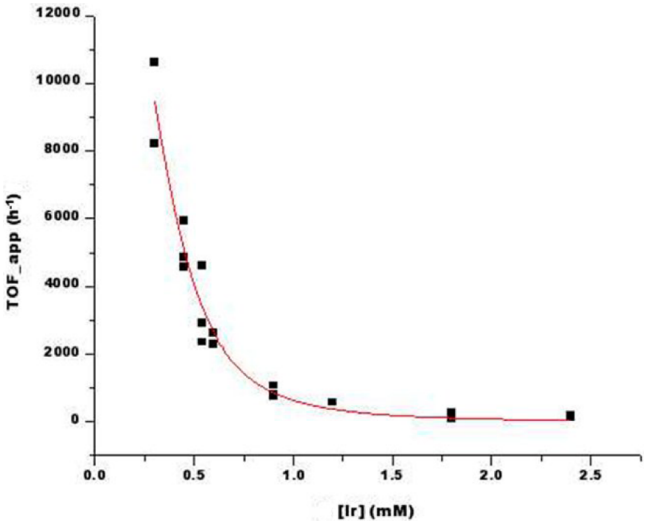

Figure 8. Nonlinear least-squares curve fit of the TOF_{app} vs [Ir] data using eq 1. The X, K_{app}, and $c{\cdot}k_{cat,2}$ constants from the fit, and as defined in Scheme 4 and by eq 1, are provided in the main text.

way, is shown in Scheme 4: basically that x equivalents of the $AlEt_3$ stabilizer dissociates in a prior equilibrium to form a more coordinatively unstaturated and therefore more active, nanoparticle (Scheme 4).

The TOF_{app} expression expected for Scheme 4 is provided in eq 1 in which $k_{cat,2} \gg k_{cat,1}$ is assumed to start (and then justified

Scheme 4. Minimum Mechanism for Hypothesis 1[a]

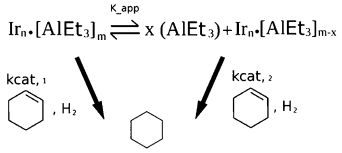

[a]Dissociation of x equivalents of $AlEt_3$ nanoparticle stabilizer via a K_{app} equilibrium constant to yield a more active, $Ir_n{\cdot}[AlEt_3]_{m-x}$ catalyst with hydrogenation rate constant $k_{cat,2}$.

ex post facto by the good fits, vide infra); see the Supporting Information for a detailed derivation of eq 1 as well as the definition of the constant, c, in eq 1. The equilibrium constant, K_{app}, in eq 1 is the $AlEt_3$ dissociation equilibrium as defined in Scheme 4, and r is the Al/Ir ratio fixed at 2.0 in the studies performed herein. TOF_{app} values are reported at $c = 1.0$ and in reduced units of hr^{-1}, that is, as $TOF_{app}(h^{-1})$; see the SI for further details.

$$TOF_{app} = c\frac{k_{cat2}K_{app}}{(r[Ir])^x + K_{app}} \quad (1)$$

Equation 1 was then curve-fit to the data using Microcal Origin 7 and nonlinear least-squares, as shown in Figure 8 (R^2 ~0.96, and the χ^2 test for goodness of fit at a given number of degrees of freedom (DOF) provided, $\chi^2/DOF \sim 411455$). The fit is quite good, accounting quantitatively for the inverse TOF_{app} vs [Ir] data. The results from the fit are (i) $x = 3.0(0.7)$, that is, on average ~3 equiv of $AlEt_3$ stabilizer dissociate from the Ir_n nanoparticle (a value of $x > 1$ was anticipated both intuitively and via simulations as being needed to provide the high curvature and overall ~127-fold increase in TOF_{app} over the 4-fold concentration range examined). The relevant fitting values and their error estimates are (ii) $K_{app} = 0.37(0.17)$; and (iii) $c{\cdot}k_{cat2} = 14800$ (4600) $hr^{-1}\ M^{(a=b)}$ (see the Supporting Information for details of the fitting procedure; the definition and molarity, $M^{(a+b)}$, units of the constant, c; and the resultant error bars[31]).

Control experiments were done next to verify the predicted decrease in the hydrogenation rate as a function of added $AlEt_3$ (i.e., and as predicted by Scheme 4 and by eq S4b of the Supporting Information which was derived on the basis of Scheme 4). The results are shown in Figure 9: the hydrogen

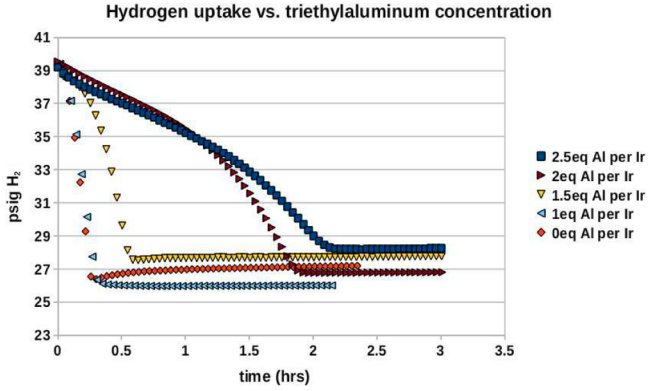

Figure 9. Control experiments demonstrating that the hydrogen uptake decreases with added $AlEt_3$, as Scheme 4 predicts.

uptake slows drastically with added $AlEt_3$ (Figure 9).[7] The data do reveal a rough k_{obs} vs $1/[AlEt_3]^{\sim 3}$ dependence over a specific concentration range, as Scheme 4 and its associated eq S4b of the SI predicts. However, any more detailed or more quantitative analysis of the data is unwarranted (and potentially misleading), since we know that a different catalyst, bulk Ir(0), forms at $AlEt_3/Ir_1$ ratios <1,[1,3,5−7] and since we also already know[1,3,5−7] that reproducible, stable nanoclusters are formed only with ≥2 equiv of $AlEt_3$.

To summarize, the attempt to try to disprove the $AlEt_3$-dissociation hypothesis by the curve fit using eq 1 and by the above added $AlEt_3$ control reactions provided, instead, strong support for the first hypothesis, consisting of a "concentration-dependent $AlEt_3$ dissociation" (Scheme 4).

(2). The Bimolecular Nanoparticle Agglomeration Hypothesis. This second hypothesis requires that higher [Ir] concentrations lead to faster, irreversible bimolecular agglomeration and, hence, increasingly larger nanoparticles at those higher concentrations (Scheme 2, part I, vide supra). To try to disprove (or support) this second hypothesis, Z-contrast STEM images were acquired on posthydrogenation catalysis samples, and the images were processed for nanoparticle size as detailed in the Experimental Section.

A representative, postcatalysis STEM image is shown in Figure 10, with this particular STEM image being for the catalyst made from 0.6 mM [Ir] precatalyst. The individual histograms for the number of particles vs particle size are summarized in the Supporting Information, and a composite histogram is provided as Figure 11.

After processing more than 600 nanoparticles, as Figure 11 shows, the average size (1.0 ± 0.3 nm diameter) of the post-catalysis nanoparticles does not change over the 0.3−2.4 mM concentration range of precatalyst examined (Figure 11). Note that the range of precatalyst concentrations corresponds to the same concentration range over which the kinetic data were obtained (Figure 8). Moreover, the unchanged particle-size

DOI: 10.1021/acscatal.5b00347
ACS Catal. 2015, 5, 3342−3353

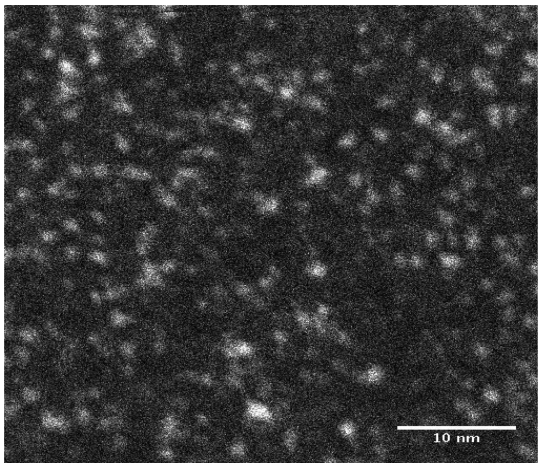

Figure 10. Z-contrast STEM image of the postcatalysis sample prepared from 0.6 mM [Ir_1] precatalyst, and where the STEM grid was prepared with sample collected after the cyclohexene hydrogenation was complete. The scale bar is 10 nm.

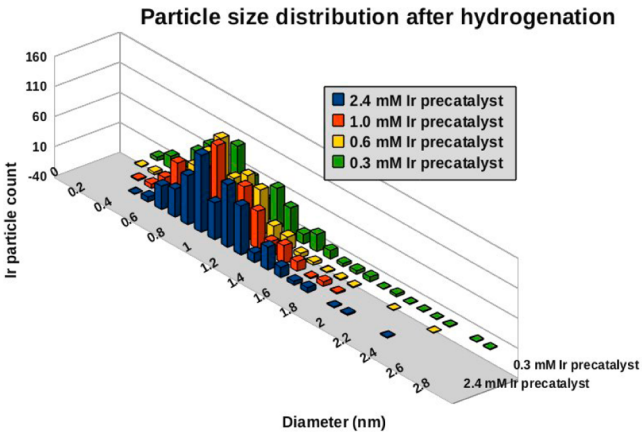

Figure 11. Particle size distribution histogram for post-hydrogenation catalysis samples, for the following [Ir] (and in parentheses the average sizes and standard deviations): 0.3 mM (1.0 ± 0.4 nm); 0.6 mM (1.0 ± 0.3 nm); 1.0 mM (1.0 ± 0.3 nm); 2.4 mM (1.1 ± 0.3 nm). The results demonstrate that no detectable change in the particle size occurs as a function of the [Ir].

results in Figure 11 are in accordance with similar findings of unchanged postcatalysis particle sizes observed as part of our earlier study.[5] Additional literature that supports in a general way the observed constant Ir_n particle sizes is also available.[32,33]

In short, irreversible bimolecular nanoparticle agglomeration is hereby disproved since no agglomeration within experimental error is seen over the range of precatalyst concentrations employed.

(3, 4). The Concentration-Dependent Fragmentation and Concentration-Dependent Size with Size-Specific Catalytic Activity Hypotheses. The third hypothesis in Table 1 is nanoparticle reversible fragmentation, wherein smaller, more active $Ir_{n/m}$ nanoparticles are formed from a larger Ir_n nanoparticle, specifically $Ir_n \rightleftarrows mIr_{n/m}$, with the smaller nanoparticles by postulate having to be considerably more catalytically active in this conceivable explanation. The fourth hypothesis couples a concentration-dependent size with a size-specific catalytic activity.

Four lines of evidence argue compellingly against these hypotheses: (i) Strong evidence exists that the *larger*, not smaller, Ziegler-type nanoparticles are the more active catalysts due to the larger particles having weaker Ir-surface ligand bonds and, thus, higher coordinative unsaturation.[5] (ii) Second, at least some change in and broadening of the nanoparticle size distribution would be expected (e.g., from the smaller $Ir_{n/m}$ formation and then its aggregation to $Ir_{2n/m}$, $Ir_{3n/m}$ plus subsequent agglomeration of these putative fragments), but none is seen by Z-contrast STEM (Figure 11, vide supra). (iii) Third, at the point where the maximum rate of hydrogen uptake and fcc $Ir(0)_{\sim 40-150}$ are both observed, 95% of the catalysis is poisoned by Hg(0),[5] consistent with the dominant catalyst being the observed, larger $Ir(0)_{\sim 40-150}$ nanoparticles. (iv) Finally, fourth and most fundamentally, such fragmentation in especially third-row metals such as Ir (i.e., where the *bulk* $Ir(0)_n$ $\Delta H_{vaporization}$ is 159 kcal/mol, leading to an average Ir−Ir bond energy of 26 kcal/mol)[34] is *energetically improbable*; this is why fragments of $Ir(0)_n$ nanoclusters are virtually without precedent, to our knowledge, and, at least in the absence of large excesses of very strong-binding ligands, able to drive the Ir−Ir cleavage.[34,35] In short, the reversible fragmentation hypothesis is not consistent with the four lines of available evidence cited.

(5). The Insidious Impurity Hypothesis, Especially Trace Water in the Case of $AlEt_3$-Stabilized Ziegler-Type Nanoparticles. The fifth and final hypothesis considered is that an insidious impurity in the present system accelerates catalysis at lower catalyst concentrations where the impurity/Ir ratio would be increasing. Water is the most obvious trace impurity and is well-known to react with $AlEt_3$ to form alumoxanes, $-(Al(Et)O)_n-$. In addition, one does expect an increasing amount of water relative to the decreasing $AlEt_3$ at lower catalyst concentrations (and for our constant Al/Ir = 2.0), despite the efforts made to minimize the H_2O in this system (efforts needed to get a catalyst with the best activity;[1] see the Experimental Section). It is also well-known that $AlEt_3$-stabilized Ziegler nanoparticle catalysts are generally water-sensitive,[1] as one would expect, but with added water typically *slowing*—not increasing—the rate of catalysis, at least with $H_2O/AlEt_3$ ratios anywhere near 1:1.[1]

The results striving to test this fifth and final hypothesis are provided in Figure S5 of the SI. (Note that the experiments performed here add water over and above the trace background water nearly unavoidably present in the system; see the Experimental Section.) The results reveal (i) a high scatter/error in the observed data (Figure S5) but that (ii) at least in the experiments performed, higher amounts of deliberately added water do tend to *slow* the TOF_{app}, as expected,[5] the *opposite trend* vs the inverse TOF_{app} vs [Ir] trend in Figure 8. Hence, there is no evidence at present in favor of this hypothesis and some evidence against it. In addition, the trace water initially present—that is, which will be reactive toward $AlEt_3$—should have already reacted with some fraction of the $2AlEt_3$ *already present*. Hence, although we do not claim to have unequivocally disproven the hypothesis of associative assistance by water in removal of the $\sim 3AlEt_3$ (and via a net initial reaction of $3/2[2AlEt_3 + 1H_2O \rightarrow 2Et-H + Et_2Al-O-AlEt_2]$), other explanations for the dissociative loss of more than a single $AlEt_3$ from the nanoparticle surface are possible, as discussed next.

The Interesting Finding of the Dissociation of ∼3 $AlEt_3$ from the $Ir(0)_{\sim 40}$ Nanoparticle Surface and Its Possible Implications. Upon reflection, the observation of the net dissociation of ∼3 $AlEt_3$, on average, from the surface of the $Ir(0)_{\sim 40}$ nanoparticle required to quantitatively fit the kinetic data is an interesting finding. One would not see such a result in, for example, a single-metal homogeneous catalyst, in which the

DOI: 10.1021/acscatal.5b00347
ACS Catal. 2015, 5, 3342−3353

sequential dissociation of ligands is typically increasingly endothermic with each ligand loss (and in the absence of major geometric and, thus, electronic reorganization post ligand loss). But, in a nanoparticle, and if the dissociation sites are far enough apart on the surface of the nanoparticle, they may behave largely independently of one another with the same effective dissociation constant—that is, the loss of ~3 $AlEt_3$ surface ligands "at once" may not only be reasonable, but may actually be a broader signature of nanoparticle (heterogeneous) catalysts vs single-metal homogeneous catalysts.

Looking at this plausible explanation for the loss of ~3 $AlEt_3$ in more detail, for the ~1.0 nm average, STEM-determined particle and thus resultant, on-average ca. $Ir_{\sim 40}$ particle, there are ~30 surface Ir for a spherical particle and thus a maximum of ~30 surface $AlEt_3$ (i.e., if one assumes for the sake of discussion a maximum of 1 $AlEt_3$ per 1 surface Ir). It is in turn at least conceivable that the 3 $AlEt_3$ binding sites that give up 1 $AlEt_3$ each could be far enough apart to act largely independently and, therefore, have approximately the same effective dissociation constant if the three surface sites in question are geometrically equivalent types of surface sites.

The above argument so noted, our intuition is that the trace, residual water unavoidably present in the (dried; see the Experimental Section) cyclohexane solvent and on the glassware surface is likely almost unavoidably involved in controlling the amount of $AlEt_3$ present in Ziegler-nanoparticle systems. Indeed, if a maximum of ~30 $AlEt_3$ can be on the ~30 surface Ir of an on-average ca. $Ir_{\sim 40}$ particle, it follows then that for the starting 2 $AlEt_3$/Ir or $2 \times 40 = 80$ $AlEt_3$ associated with a single $Ir_{\sim 40}$ particle, that 80−30 = 50 $AlEt_3$ would have to be in solution or somehow "missing". Important to note here is that Scheme 4 does not show any starting $AlEt_3$ on the right-hand side of the dissociative K_{app} equilibrium, yet Scheme 4 and its associated eq 1 provide an excellent, quantitative curve fit of the observed data in Figure 8. The implication from the kinetics is that the other ~50 $AlEt_3$ are effectively "not there", quite plausibly having been consumed by trace H_2O and acting as the "final drying agent" in the system.

Confirming or refuting this hypothesized role of H_2O will require additional studies, with absolute control over the amount of water present and independent determination of the amount of water and $AlEt_3$ present in operando and, hence, the precise role of the water in $AlEt_3$-stabilized Ziegler-type nanoparticles. Such studies are beyond the scope of the present work, the goal of which was to test the five alternative hypotheses for the inverse TOF_{app} vs [precatalyst or catalyst] data and to provide a disproof-based, quantitative-fit explanation for that data. Scheme 4 and the quantitative fit in Figure 8 achieve that goal and even begin to offer some quantitative suggestions about the fate and locale of the originally added $AlEt_3$.

Analysis of the Literature TOF_{app} vs [Co] Data for Co-Based Zeigler-Type Subnanometer Cluster Catalysis. The closest analogue to our Ir/$AlEt_3$ system in the extant Ziegler nanocluster literature[1] comes from the published, important work of Shmidt and co-workers.[14] Their $Co(acac)_2$/$AlEt_3$-based catalyst system also employs a metal in the Co, Rh, Ir group and utilizes the same $AlEt_3$ stabilizer. They, too, see the same inverse trend as mentioned in the Introduction and Figure 4 (vide supra) and attributed it to agglomeration, but did not provide any quantitative fit to the observed kinetic data.[14] It was of some interest, therefore, as a test of the broader applicability of our results to try to fit our $AlEt_3$ dissociative equilibrium mechanism to their data[14] using our eq 1.

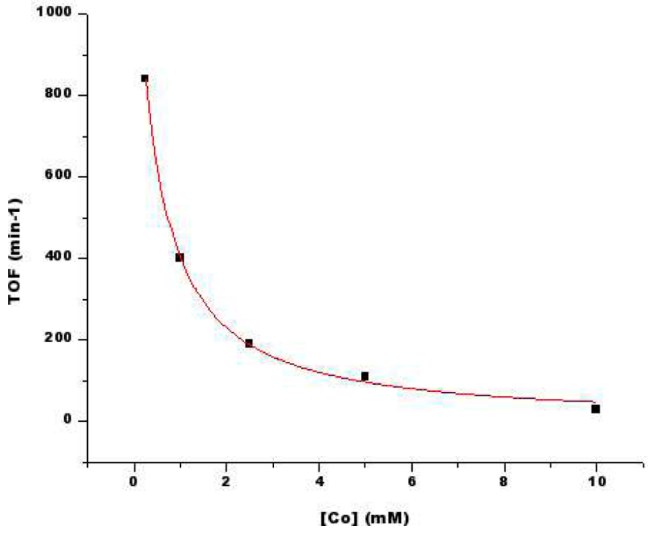

Figure 12. Fitting of Nindakova et al.'s 1-hexene hydrogenation data,[14] for their $Co(acac)_2$/$AlEt_3$-based catalyst in heptane, to the $AlEt_3$ dissociative mechanism and its associate eq 1. The resulting constants are k_{cat2} = 1217(153), K_{app} = 1.05(32), and the stabilizer dissociation number is x = 1.09(12).[14] Clearly, the $AlEt_3$ dissociative scheme uncovered herein and its associated eq 1 provide an excellent fit. That said, a more detailed interpretation of what this empirical fit means physically and mechanistically must await the following information, which is unclear from the published paper:[14] what precise Al/Co ratio was used in this study; is that ratio changing as the [Co] changes; and which of the two precatalysts (differing in their water content) was used, $Co(acac)_2 \cdot nH_2O$, n = ~2 or the n = 0 complex.[14]

The needed data analysis and curve fit are shown in Figure 12. The fit again *quantitatively reproduces the observed inverse curve* (Figure 12), with the resultant constants (and error estimates)—k_{cat2} = 1217(153), K_{app} = 1.05(0.32)—and average number of dissociated stabilizer molecules, x = 1.09(0.12).[31] Hence, it is clear that the $AlEt_3$ dissociative mechanism uncovered herein quantitatively fits this second system with its independent data, as well. Noteworthy here is that cobalt is the basis of the current, industrially preferred, polymer hydrogenation catalyst.[1]

The effect of added water in the classic $Co(acac)_2$/$AlEt_3$-based catalyst is interesting, as well.[14] Starting with a $Co(acac)_2 \cdot nH_2O$ (n = ~2) precursor requires ~8 $AlEt_3$/1 Co for maximum styrene hydrogenation catalytic activity in toluene. That system also gives a catalyst ~2-fold more active than that prepared using a no deliberately added water, $Co(acac)_2 \cdot nH_2O$ (n = 0) precatalyst, the latter requiring only ~4 $AlEt_3$/1 Co to reach its maximum (but 2-fold lower) catalytic activity (see Figure 1 in that work).[14] These experiments, in which ~2 equiv of water require 4 more equiv of $AlEt_3$, provide excellent evidence for the (expected) quantitative reaction of water with $AlEt_3$ in these systems via the implied, initial 2:1 stoichiometry of $2AlEt_3 + 1H_2O \rightarrow 2Et\text{-}H + Et_2Al{-}O{-}AlEt_2$.

The above results are also supportive in a general way of the finding in the Ir system in which around half (there, ~50/80) of the added $AlEt_3$ "goes missing" kinetically, quite plausibly due to reaction with residual H_2O under the specific, millimolar [precatalyst] concentrations employed in the Ir studies.

SUMMARY AND CONCLUSIONS

The following are the main conclusions from this study:

- The observation of an inverse TOF vs [precatalyst or catalyst] curve has been seen eight times in the literature,

DOI: 10.1021/acscatal.5b00347
ACS Catal. 2015, 5, 3342−3353

leading to five suggested explanations for its underlying cause, as summarized back in Table 1. However, a detailed test of these possible explanations has not previously appeared.

- A new alternative hypothesis compared to any present in the literature has been postulated herein for the observed inverse TOF_{app} vs [Ir] dependence, namely, a "concentration-dependent $AlEt_3$ stabilizer dissociative equilibrium". Five total alternative hypotheses were then tested for the first time.
- Of the five hypotheses tested, only the $AlEt_3$ stabilizer dissociative equilibrium hypothesis is able to account for the $[(1,5\text{-COD})Ir(\mu\text{-}O_2C_8H_{15})]_2$ plus $AlEt_3$ system data. Moreover, the proposed minimal mechanism and associated kinetic equation, Scheme 4, are able to account quantitatively for the observed inverse TOF_{app} vs [Ir] kinetic data.
- The $AlEt_3$ stabilizer dissociative equilibrium hypothesis was also able to account quantitatively for an analogous inverse TOF_{appt} vs [precatalyst] dependence for a literature $Co(acac)_2/AlEt_3$ system studied by Nindakova, Shmidt and co-workers in their classic work.[14] However, additional details of that study (specifically, the amount of water, *n*, in the precatalyst $Co(acac)_2{\cdot}nH_2O$ and the Al/Co ratio for each data point) will be needed before a more detailed interpretation of the curve fit in Figure 12 can be made.
- The present study suggests, then, anytime an inverse dependence of TOF_{appp} on [precatalyst or catalyst] is seen, that (i) the five hypotheses in Table 1 should be tested (i.e., if applicable to the system at hand, plus, of course, any others that are reasonable for or relevant to that particular system); but that (ii) hypothesis I in Table 1, of a concentration dependence of some reagent in the underlying, incompletely understood rate law, should be a first, obvious hypothesis tested for the observed inverse dependence. After all, a TOF_{app} measurement is a kinetic measurement, so that until a true, constant TOF is obtained (i.e., a TOF based on a *rate constant*), one pretty much has to be measuring some incompletely understood part of the underlying rate law!
- The kinetic effect on the TOF_{app} can be significant, for example, by a factor of ~127 over the concentration range studied herein. Even factors of 10 are industrially significant in the throughput of hydrogenated polymer using Ziegler-nanoparticle catalysts, why, for example, cobalt replaced the earlier nickel-based commercial catalysts.[1,4]
- The present studies also bear heavily on the current, unnecessary controversy over the use of the TOF concept in catalysis.[36−39] In particular, the present studies emphasize that the use of, and especially the (cautious!) comparison of, TOFs makes sense *only when the full rate law for the catalytic process(es) at hand is(are) known*.[36] When one has, instead, TOF_{app} values that contain underlying concentration terms from the (often unknown) fuller rate law, then comparison of those TOF_{app} values—with their then different, often hidden, units!—is an unwitting comparison of different (unknown) rate laws as well as different concentration terms in those (different) rate laws, a truly unwise, "apples and oranges" comparison. Such unwitting comparisons can only result in generally incorrect, misleading conclusions and resultant confusion. The use of the *apparent* turnover frequency, TOF_{app}, as employed herein, and awareness of its units from the rate law, are two small but very useful tools for avoiding future problems and confusion when presenting and discussing turnover frequency data in catalysis.

EXPERIMENTAL SECTION

Materials. All materials were handled and stored in a Vacuum Atmospheres N_2 filled drybox. The O_2 level in the drybox was monitored by a Vacuum Atmospheres O_2 sensor and kept between 0.4 and 5 ppm (usually less than 1 ppm). Glassware was cleaned and dried overnight in an oven set to 160 °C then loaded into the Vacuum Atmospheres antechamber and pumped down to 30 psi below atmospheric pressure. The antechamber was then purged twice with N_2 gas (10 min to pump down between purge cycles, 30 min total) prior to transfer of glassware into the drybox. Cyclohexane (Sigma-Aldrich 99.5%) was kept over 4 A molecular sieves (Acros Organics, activated in the same oven via heating at 160 °C for more than 3 days). Cyclohexene (Sigma-Aldrich, 99%, ReagentPlus, inhibitor free) was purified using an Innovative Technology PureSolv Micro solvent purification system equipped with an activated alumina column. $AlEt_3$ (Strem Chemicals, 93%) was used as received. *Caution!* Trialkylaluminum is extremely pyrophoric and must be handled using air and moisture-free techniques.[40] $AlEt_3$ ignites spontaneously when in contact with air. As with all pyrophoric reagents, $AlEt_3$ is more dangerous when flammable solvents are present (e.g., the cyclohexane solvent employed herein). Hence, the required safety considerations were carefully designed and followed, including: (i) first reading the MSDS safety sheet on $AlEt_3$; (ii) working with the minimal amounts of pyrophoric and flammable reagents possible; (iii) using the $AlEt_3$ only in a drybox or in a Fisher-Porter (FP) bottle that was sealed using Swagelock quick-connects and under a under N_2 atmosphere before taking the FP bottle out of the drybox.

The dark red precatalyst $[(1,5\text{-COD})Ir(\mu\text{-}O_2C_8H_{15})]_2$ was prepared as previously reported[41] and used as prepared once its purity had been verified by NMR.[41]

Apparatus. Catalytic hydrogenation was performed in an apparatus (that is detailed in our previous literature[42]) composed of a hydrogen tank (Airgas HY300) with a pressure regulator (Airgas Y12-D244D) set to 40 psi connected to (i) a moisture trap (Trigon Technologies TTM400-4), (ii) an oxygen trap (Trigon Technologies TTO-100-4), (iii) an indicating oxygen trap (Trigon Technologies TTIO-150-4), (iv) a rotary-vane vacuum pump (Welch DirecTorr 8925, 1×10^{-4} Torr ultimate pressure), (v) Swagelok quick-connects, (vi) a Fisher-Porter bottle (Andrews Glass 3 oz PRV), and (vii) a pressure transducer (Omega PX624) powered by an Omega PSS D15C 15 V power supply and interfaced to a PC via an RS232 interface provided by an Omegabus D1131 (A/D converter). Swagelok valves are part of the apparatus which allows (a) isolation of the H_2 tank and traps from the quick connects; (b) the ability to switch from adding hydrogen to the Fisher-Porter (FP) bottle to, instead, vacuuming the FP bottle out; (c) the ability to vacuum the quick connect system itself; and (d) the ability to purge with H_2 the N_2 gas initially in the FP bottle. A drawing of nearly identical apparatus is available in a previous publication.[42] Also part of the hydrogenation system is a ±0.1 °C temperature control system consisting of a recirculating water bath (VWR) connected to a 250 mL bath (Wilmad Lab Glass) that was filled halfway with light mineral oil (Fisher O121-1) and placed on top of a heavy-duty Fauske Super Magnetic Stirrer. The Fisher-Porter bottle is immersed deep enough in mineral oil, by a factor of 2 or 3 in terms of the height of the oil

DOI: 10.1021/acscatal.5b00347
ACS Catal. 2015, 5, 3342−3353

being above the height of the reacting solution, to cover the solution undergoing catalytic hydrogenation.

Stock Solutions. "Concentrated stock" solution, 360 mM $AlEt_3$, was prepared in the drybox by transferring (liquids, by syringe unless otherwise noted) 0.53 mL of $AlEt_3$ into 2 mL of dried cyclohexane then diluting to the 10 mL mark of a volumetric flask with dried cyclohexane. "Regular stock" solution, 36.0 mM $AlEt_3$, was prepared by transferring 2.5 mL of the "concentrated stock" solution to a 25 mL volumetric flask and diluting with dried cyclohexane to the mark. "Precursor stock" solution, 3.6 mM $[(1,5\text{-COD})Ir(\mu\text{-}O_2C_8H_{15})]_2$ (and therefore twice this, 7.2 mM in [Ir]) was prepared by weighing out 31.9 mg (0.036 mmol) of the dark-red crystalline solid $[(1,5\text{-COD})Ir(\mu\text{-}O_2C_8H_{15})]_2$ in a 5 mL glass vial and transferring (via a pyrex weighing funnel) to a 10 mL volumetric flask and diluting to the mark with dried cyclohexane.

Catalytic Hydrogenations and Reporter Reaction. Catalytic hydrogenations and the underlying catalyst formation were monitored by our previously published cyclohexene hydrogenation reporter reaction method.[11] The Fisher-Porter bottle to be used in the catalytic hydrogenations was cleaned (1−5 mL soap and then >1000 mL distilled water) then dried in an oven at 160 °C for more than 24 h. The FP bottle was then transferred into the drybox, after which a new 22 × 175 mm Pyrex culture tube containing a new 5/8 × 5/16 in. Teflon-coated magnetic stir bar was placed inside the FP bottle. The culture tube was filled with a precatalyst solution of the desired concentration. The FP bottle was then sealed, removed from the drybox, and connected to the Swagelok quick connects via a T-shaped system of Swagelok valves.

Specifically, to prepare a 1.2 mM solution of [Ir] in cyclohexane with an Al/Ir ratio of 2.0: (i) 0.50 mL of "precursor stock" solution (7.2 mM [Ir]) was transferred to the culture tube; (ii) 1.80 mL of cyclohexane was added; (iii) 0.20 mL of $AlEt_3$ stock solution (36.0 mM in cyclohexane) was then added in a rapid dropwise manner (∼2 drops/sec); (iv) the solution was aged (aging of the catalyst was previously found to be key, since the catalytic activity varies with aging time, becoming linear near 9 h)[5] under vortex stirring for 9 h; and (v) 0.5 mL of cyclohexene was added (total volume now 3.0 mL). The culture tube was placed inside the FP bottle and sealed (with the Andrews Glass PRV coupling) to the system of Swagelok valves and quick-connects. This sealed FP was then transferred outside the drybox and attached to the hydrogenation apparatus (via Swagelok quick connects described previously); 1000 rpm stirring was then started. The quick-connects, valves, and nylon tubing lines were then vacuumed for 4 min, then the solution was exposed to hydrogen at ∼40 psig for 15 s, at which time a valve was opened for ∼0.5 s to purge the gas above the catalytic solution. This "purge cycle" was repeated 15 times, then 30 s was allowed to pass before isolating the reaction from the H_2 tank (so that H_2 consumption could be monitored). LabVIEW 8.2 was used to collect this hydrogen consumption monitored as a decrease in pressure on the PC and the data were saved in the well-known "CSV" format.

Kinetic Data Analysis. The CSV format hydrogenation kinetic data from LabVIEW was processed using a GNU Octave script written for the purpose (see the Supporting Information for details), then viewed and additionally processed in OpenOffice 3.2. Because the kinetic curves typically exhibited an induction period (see Figure 7, vide supra), multiple ways of treating the data were tested initially, including using the maximum rate as employed before[5] (see the Supporting Information for further details). However, using the simple average rate of hydrogen consumption over the whole run proved both sufficient and justifiable as the representative rate over the whole hydrogenation. The average rate was obtained straightforwardly by subtracting the minimum pressure from the maximum pressure and dividing this difference by the total hydrogenation time, but while still using the GNU Octave script described in the SI. The resultant average rate of H_2 loss, in units of psig/h, was converted to an average rate of cyclohexene loss by multiplying by a conversion constant specific to our apparatus (125 mM cyclohexene/psig H_2) that involves knowing the total gas volume of our system, PV = *nRT*, and the well-established 1:1 cyclohexene/H_2 stoichiometry (see also the "Hydrogen Reservoir"[43] concept presented elsewhere if additional details are required).

The TOF_{appt} (hr^{-1}) = (average rate/[Ir])·4/3 was calculated according to the indicated equation as follows: The average rate value (units of mM/h) was then converted to a TOF_{app} (units hr^{-1}) by dividing by the [Ir] (units of mM) used for that particular run while also correcting for the available surface iridium for the average, ∼1 nm, $Ir_{\sim 40}$ clusters. This correction was made by dividing the denominator by 30/40 (i.e., multiplying by 40/30), this ∼3/4 value being the fraction Ir atoms on the surface in a ∼1 nm, $Ir_{\sim 40}$ average-size cluster. The result is a TOF_{appt} (hr^{-1}) based on the surface-available Ir.

Z-Contrast STEM. For each catalyst studied, the FP bottle was detached from the hydrogenation line and returned to the drybox, and the sample was diluted to twice its original volume. After completion of the catalytic runs, the vials were sealed airtight, as reported previously.[3] The catalyst samples were prepared at Colorado State University (CSU), sealed airtight, and then shipped to the University of Pittsburgh for Z-contrast STEM imaging. Grid preparation for Z-contrast microscopy was conducted in an N_2 filled glovebag. Briefly, two or three drops of each catalyst solution was dispersed onto a TEM grid consisting of an ultrathin carbon film on a holey carbon support (Ted Pella, Inc.). Grids were then dried at room temperature and then transferred quickly into the TEM column. Images were acquired using a Hitachi HD-2300 field-emission scanning transmission electron microscope operating at 200 kV. The samples were treated with a high-intensity electron beam (electron beam shower) for ∼15 min each time in the TEM column (pressure $<3 \times 10^{-6}$ Torr) to assist in high-quality imaging (Ir−Ir bonds, as reported here and previously,[5] appear to generally be stable under these characterization conditions). The high-angle scattering electrons were collected with a JEOL ADF detector at a camera length of 8 cm, with a 0.2 nm (nominal) diameter probe.

STEM Data Analysis. Z-contrast STEM images were processed by a hand-counting procedure that utilizes two Gaussian fits to each observed particle. The particle diameter is given as fwhm of the fit Gaussian[44] (see the Supporting Information for additional details on the particle counting methodology).

Water Addition Experiments. Following the same general procedure for making solutions as in the section on Catalytic Hydrogenations and Reporter Reaction, a solution 1.2 mM in [Ir] and at a 2/1 $AlEt_3$/Ir ratio was made up as follows: In the drybox, 0.50 mL of a stock (7.2 mM [Ir_1]) solution was added to, respectively, 1.7, 1.6, 1.4, or 1.3 mL cyclohexane in new 22 × 175 mm Pyrex culture tubes containing new 5/8 × 5/16 in. Teflon-coated magnetic stir bars (so that the total volume always summed to 3.0 mL, vide infra). This was followed by the addition of 0.20 mL of 36.0 mM $AlEt_3$ and then by 0.5, 1.0, 2.0, and 5.0 equiv of H_2O per mole of Al (as 0.1, 0.2, 0.4, 0.5 mL of a 36 mM H_2O solution in cyclohexane) using a 1.0 mL syringe, with the

DOI: 10.1021/acscatal.5b00347
ACS Catal. 2015, 5, 3342−3353

total volume equaling 3.0 mL in each of the four, individual experiments when 0.5 mL cyclohexene was added. (The maximum solubility of H_2O in cyclohexane at 25 °C is 0.01 g H_2O/100 g cyclohexane, or 50 mM according to an IUPAC-NIST database[45]). The solution was aged with stirring for 9 h while still in the drybox. Then, 0.5 mL of cyclohexene was added, and the culture tube was placed in a FP bottle, sealed, removed from the drybox, and connected to the hydrogenation line via the quick-connects, and a hydrogenation started as detailed under the Catalytic Hydrogenations and Reporter Reaction section. Each experiment was repeated at least twice, and the results are reported in Figure S4 of the SI.

■ ASSOCIATED CONTENT

Supporting Information

The following file is available free of charge on the ACS Publications website at DOI: 10.1021/acscatal.5b00347.

NMR of the precatalyst demonstrating its purity; details of processing the hydrogenation reporter reaction kinetic data; derivation of the kinetic equation used in the curve fitting; STEM image processing details and particle size distributions; particle counting methodology; individual particle-size histograms; and Figure S5 showing the added water experiments (PDF)

■ AUTHOR INFORMATION

Corresponding Author

*E-mail: rfinke@lamar.colostate.edu.

Notes

The authors declare no competing financial interests.

■ ACKNOWLEDGMENTS

This work was supported by NSF Grant CHE-0611588 and DOE BES Grant DE-FG02-03ER15476. L. Li and J. C. Yang thank RJ Lee Group, Inc. for use of their TEM facilities. Dr. William Morgan Alley is acknowledged for performing early experiments in this work.

■ REFERENCES

(1) Alley, W. M.; Hamdemir, I. K.; Johnson, K. A.; Finke, R. G. *J. Mol. Catal. A: Chem.* **2010**, *315*, 1−27.

(2) Alley, W. M.; Girard, C. W.; Özkar, S.; Finke, R. G. *Inorg. Chem.* **2009**, *48*, 1114−1121.

(3) Alley, W. M.; Hamdemir, I. K.; Wang, Q.; Frenkel, A. I.; Li, L.; Yang, J. C.; Menard, L. D.; Nuzzo, R. G.; Özkar, S.; Yih, K.-H.; Johnson, K. A.; Finke, R. G. *Langmuir* **2011**, *27*, 6279−6294.

(4) Johnson, K. A. *Polym. Prepr. (Am. Chem. Soc., Div. Polym. Chem.)* **2000**, *41*, 1525−1526.

(5) Alley, W. M.; Hamdemir, I. K.; Wang, Q.; Frenkel, A. I.; Li, L.; Yang, J. C.; Menard, L. D.; Nuzzo, R. G.; Özkar, S.; Johnson, K. A.; Finke, R. G. *Inorg. Chem.* **2010**, *49*, 8131−8147.

(6) Hamdemir, I. K.; Özkar, S.; Yih, K.-H.; Mondloch, J. E.; Finke, R. G. *ACS Catal.* **2012**, *2*, 632−641.

(7) Hamdemir, I. K.; Özkar, S.; Finke, R. G. *J. Mol. Catal. A: Chem.* **2013**, *378*, 333−343.

(8) Crabtree, R. H. *Chem. Rev.* **2012**, *112*, 1536−1554.

(9) Schwartz's definition also refers to the homogeneity or heterogeneity of the catalyst active sites, not the solubility of the catalyst, see: (a) Schwartz, J. *Acc. Chem. Res.* **1985**, *18*, 302−308. See also: (b) Collman, J. P.; Hegedus, L. S.; Norton, J. R.; Finke, R. G. *Principles and Applications of Organotransition Metal Chemistry*; University Science Books: Mill Valley, CA, 1987; pp 561−562. (c) Widegren, J.; Finke, R. *J. Mol. Catal. A: Chem.* **2003**, *198*, 317−341.

(10) (a) Ott, L. S.; Finke, R. G. *Coord. Chem. Rev.* **2007**, *251*, 1075−1100. (b) Interestingly, our prior literature review of nanocluster stabilizers[10a] reveals little prior precedent for Lewis acids such as $AlEt_3$ as nanoparticle stabilizers, much less as the superior nanoparticle stabilizers that $AlEt_3$ has been shown to be.[10b].

(11) Mondloch, J. E.; Wang, Q.; Frenkel, A. I.; Finke, R. G. *J. Am. Chem. Soc.* **2010**, *132*, 9701−9714.

(12) (a) Bartholomew, C. H.; Farrauto, R. J. *Fundamentals of Industrial Catalytic Processes*; 2nd ed.; Wiley: Hoboken, NJ, 2006; Chapter 5, p 261. (b) As noted by Bartholomew[12a] (see also Boudart's original work[39]), "The turnover frequency (TOF) is a specific reaction rate based on the number of active sites." The authors further specify that the "specific reaction rate" = $1/(\nu Q) \times d[n]/dt$ where ν is the stoichiometric coefficient in the reaction; n is the number of moles of the species; t is time; and Q is the volume, weight, or surface area of the catalyst. Units are molecules/site-second or 1/s.

(13) Smirnov, V. V.; Tarkhanova, I. G.; Kokorin, A. I.; Tsvetkov, D. S. *Kinet. Catal.* **2005**, *46*, 861−866.

(14) Nindakova, L. O.; Shmidt, F. K.; Saraev, V. V.; Shainyan, B. A.; Chipanina, N. N.; Umanets, V. A.; Belonogova, L. N.; Toryashinova, D.-S. D. *Kinet. Catal.* **2006**, *47*, 54−63.

(15) Shmidt, F. K.; Nindakova, L. O.; Shainyan, B. A.; Saraev, V. V.; Chipanina, N. N.; Umanetz, V. A. *J. Mol. Catal. A: Chem.* **2005**, *235*, 161−172.

(16) Steinhoff, B. A.; Fix, S. R.; Stahl, S. S. *J. Am. Chem. Soc.* **2002**, *124*, 766−767.

(17) Sanchez-Delgado, R. A.; Andriollo, A.; Puga, J.; Martin, G. *Inorg. Chem.* **1987**, *26*, 1867−1870.

(18) D'Ornelas, L.; Choplin, A.; Basset, J. M.; Puga, J.; Sanchez-Delgado, R. A. *Inorg. Chem.* **1986**, *25*, 4315−4316.

(19) Fairlamb, I. J. S.; Kapdi, A. R.; Lee, A. F.; Sanchez, G.; Lopez, G.; Serrano, J. L.; Garcia, L.; Perez, J.; Perez, E. *Dalton Transactions.* **2004**, 3970−3981.

(20) Reetz, M. T.; De Vries, J. G. *Chem. Commun.* **2004**, 1559−1563.

(21) De Vries, A. H. M.; Mulders, J. M. C. A.; Mommers, J. H. M.; Henderickx, H. J. W.; De Vries, J. G. *Org. Lett.* **2003**, *5*, 3285−3288.

(22) Schmidt, A. F.; Smirnov, V. V. *Top. Catal.* **2005**, *32*, 71−75.

(23) Watzky, M. A.; Finke, R. G. *J. Am. Chem. Soc.* **1997**, *119*, 10382−10400.

(24) (a) Watzky, M. A.; Finney, E. E.; Finke, R. G. *J. Am. Chem. Soc.* **2008**, *130*, 11959−11969. (b) When the Finke−Watzky (F−W) two step (A → B, A + B → 2B) slow, continuous nucleation and autocatalytic surface-growth mechanism of nanoparticle formation[23] is followed, then a size vs time relationship can be derived for transition metal nanoparticles, as done in the above cited publication.[24] However, lower concentrations often yield fewer nuclei, and that tends to make larger, not smaller, particles.

(25) (a) Surface atoms of nanoparticles (when compared to bulk transition metal) have less coordinative saturation and possess additional free energy. For this reason, variation in size-specific activity of nanoparticles is expected. Another simple way to understand this effect is that the $\Delta H_{vaporization}$ of bulk $Ir(0)_n$ to nIr(0) atoms requires 159 kcal/mol. This fact teaches that until sufficient Ir−Ir metal, metal bonding is achieved in increasingly larger particles, that *at least unligated, naked* smaller particles should generally be of higher free energy vs their larger counterparts and, therefore, potentially of higher catalytic activity. Ligand effects can reverse this trend, however, so that the opposite is actually seen for $Ir(0)_n$ nanocluster hydrogenation catalysts, the larger particles typically being more active.[25b,c] (b) Besson, C.; Finney, E. E.; Finke, R. G. *J. Am. Chem. Soc.* **2005**, *127*, 8179−8184. (c) Besson, C.; Finney, E. E.; Finke, R. G. *Chem. Mater.* **2005**, *17*, 4925−4938.

(26) Zhou, X.; Xu, W.; Liu, G.; Panda, D.; Chen, P. *J. Am. Chem. Soc.* **2009**, *132*, 138−146.

(27) A version of the size-dependent catalytic activity hypothesis is "The Magic Number Nanoclusters Hypothesis". In a Heck reaction with aryl bromides, Schmidt (aka Shmidt[15]) and Smirnov[22] found higher-order aggregation with respect to Pd(0) concentration insufficient to explain their inverse kinetics since their reaction becomes negative order in Pd at a specific concentration interval, 0.8−3.2 mM. Schmidt and

DOI: 10.1021/acscatal.5b00347
ACS Catal. 2015, 5, 3342−3353

Smirnov instead explained their inverse TOF vs [Pd] in terms of closed shell, or "magic number," nanoparticles where such full shell nanoparticles are known to be more stable at the "magic numbers" of (M = metal) M_{13}, M_{55}, M_{147}, M_{309}, M_{561}, M_{923}, and so on. A corresponding increase in activity and, thus, TOF_{app}, is therefore plausible between two given magic numbers as surface shell saturation decreases. Hence, the "magic number hypothesis", a version of the size-dependent activity hypothesis, is another plausible hypothesis. However, (i) this alternative hypothesis can be ruled out *for the present Ir(0) system* by the constant, ∼1.0 nm Ir(0) nanoparticle size seen herein (Figure 11). Moreover, two differences immediately apparent when comparing the data for the present Ir(0) Ziegler-nanoparticle system (Figure 3) vs that for the $Pd(0)_m$ system (Figure 5) are (ii) that an up-turn in the reaction rate at higher starting Pd(II) concentrations is seen for the $Pd(0)_m$ (see Figure 1 elsewhere[22]), but is not seen for the present $Ir(0)_n$ Ziegler-nanoparticle system (Figure 3 herein); and (iii) the magnitude of the maximum rise in the TOF of Figure 1 elsewhere is less than 4-fold, vs an 11-fold maximum rise for the present Ir(0) system (when plotted as rates instead of TOF's so that a comparison can be made with the $Pd(0)_m$ system). Hence, for the "magic number sizes" hypothesis to be supported for even the Pd(0) work,[22] the following are minimally required: (a) disproof of the nanoparticle ligand dissociative equilibrium finding uncovered herein (with, perhaps, an added first-order process in [Pd(II)] being added to try to account for the up-turn in Figure 1 elsewhere[22] at higher [Pd(II)]), and (b) definitive evidence for or against changing particle sizes as a function of the starting [Pd(II)].

(28) (a) For a lead reference, see the following and references therein: Doll, K. M.; Finke, R. G. *Inorg. Chem.* **2004**, *43*, 2611−2623. (b) See also the discussion of trace impurities, as well as the other valuable hints for performing kinetic studies, in *Investigations of Rates and Mechanisms of Reactions*; Bernasconi, Ed.; Wiley: New York, 1986; Vol. *VI*, p 238.

(29) Byrd, J. E.; Wilmarth, W. K. *Inorg. Chim. Acta, Rev.* **1971**, *5*, 7−18.

(30) Malin, J. M.; Toma, H. E.; Giesbrecht, E. *J. Chem. Educ.* **1977**, *54*, 385.

(31) The first uncertain digit is the last significant one, however, and as often done, to mitigate against round-off errors when used in subsequent calculations, the values reported carry an additional (formally nonsignificant) figure.

(32) (a) Pawluk, T.; Hirata, Y.; Wang, L. *J. Phys. Chem. B* **2005**, *109*, 20817−20823. (b) The DFT calculations performed by Pawluk et. al[32a] on naked, unligated Ir particles are also consistent with the constant particle sizes observed. Specifically, Pawluk and co-workers find that (naked; unligated) Ir particles prefer a simple cubic structure until a 48 atom particle (5.91 eV per Ir atom binding energy) is reached, at which point the transition to face-centered cubic occurs. This 48 atom (about 1.1 nm diameter) limit restricts coalescence of at least naked, smaller nanoparticles because energetically unfavorable surface rearrangements would be required, again with the caveat here that these calculations refer strictly to only naked, unligated Ir nanoparticles.

(33) Aydin, C.; Lu, J.; Browning, N. D.; Gates, B. C. *Angew. Chem., Int. Ed.* **2012**, *51*, 5929−5934.

(34) Uzun, A.; Gates, B. C. *Angew. Chem., Int. Ed.* **2008**, *47*, 9245−9248.

(35) Worth nothing here is that when we wrote our 2003 review of the "Is it homogeneous or heterogeneous catalysis?" question and problem,[9c] we noted, as a final point in the summary (see p. 334)[9c] that "more information is needed about the $M_n + (x - m)L \; M_{n-} + mML_x$ equilibrium as a function of the specific L, bidendate L−L, and temperature ... ". This statement is still true in 2015.

(36) Kozuch et al.[37] and Lente[38] have recently discussed the care that must be exercised when interpreting TOF.[39] The present work confirms a key point: the use of, and especially the comparison of, TOFs—often *really* TOF_{app} *values*—makes sense only when the rate law for each system being compared is known.

(37) Kozuch, S.; Martin, J. M. *ACS Catal.* **2012**, *2*, 2787−2794.

(38) Lente, G. *ACS Catal.* **2013**, *3*, 381−382.

(39) For a classic contribution on the definition and proper use of TOF in catalysis, see: Boudart, M. *Chem. Rev.* **1995**, *95*, 661−666.

(40) Shriver, D. F.; Drezdzon, M. A. *The Manipulation of Air-Sensitive Compounds*; Wiley: New York, 1986; Chapters 1−4, pp 1−86.

(41) Yih, K.-H.; Alley, W. M.; Finke, R. G. *Organometallics* **2011**, *30*, 5068−5070.

(42) Aiken, J. D., III; Finke, R. G. *J. Am. Chem. Soc.* **1998**, *120*, 9545−9554.

(43) (a) Lin, Y.; Finke, R. G. *Inorg. Chem.* **1994**, *33*, 4891−4910. See p. 4906, left-hand column where "The *apparent turnover rate*..." is discussed. (b) See also the concept of a "Hydrogen Reservoir", as discussed in the two Ph.D. theses listed as references 8 and 9 in this 1994 paper.[43]

(44) Lu, J.; Serna, P.; Aydin, C.; Browning, N. D.; Gates, B. C. *J. Am. Chem. Soc.* **2011**, *133*, 16186−16195.

(45) Maczynski, A.; Shaw, D. G. *J. Phys. Chem. Ref. Data* **2005**, *34*, 657−708 see p. 675.

DOI: 10.1021/acscatal.5b00347
ACS Catal. 2015, 5, 3342−3353